I. J. Insect Morphol. & Embryol., Vol. 9, pp. 281 to 296.

0020-7322/80/0801-0281$20.00/0

FINE STRUCTURE OF THE BEAN-SHAPED ACCESSORY GLAND IN THE MALE PUPA OF *TENEBRIO MOLITOR* L. (COLEOPTERA : TENEBRIONIDAE)*

MARGARET J. GRIMES and GEORGE M. HAPP†

Department of Zoology and Entomology, Colorado State University, Fort Collins, CO 80523, U.S.A.

†Department of Zoology, University of Vermont, Burlington, VT 05405, U.S.A.

(*Accepted* 25 *February* 1980)

Abstract—The bean-shaped accessory glands of the mealworm beetle, *Tenebrio molitor* L., produce secretions that form the outer layers of the spermatophore. We aim to understand the hormonal control of growth and differentiation of these glands. In the present paper, we describe the morphology of the glands during pupal maturation *in situ*. The primary ultrastructural changes during development are those related to the maturation of the secretory machinery, including an increase in prominence of the nucleoli, the expansion of the rough endoplasmic reticulum and Golgi complexes, and tracheolar invaginations into the glandular epithelium. These glands increase in size due to cell division, and undergo a change in shape from oval to reniform due to differential mitotic rates in different regions. Of particular interest are cytoplasmic bridges between apposed cells. Although most common during the peak period of cell division, these bridges are not merely relics of incomplete cytokinesis but are potential sites for intercellular communication. The study has provided useful indices for scoring the progressive differentiation of the bean-shaped glands.

Index descriptors (in addition to those in title): Mealworm beetles, intercellular bridges, polyploidy, mitotic rates.

INTRODUCTION

ACCESSORY reproductive glands are common among male insects, except for some Apterygota and Diptera (Richards and Davies, 1977). These glands have been widely studied because of their importance for many species in achieving successful fertilization (for review, see Leopold, 1976). In the mealworm beetle, *T. molitor*, there are 2 pairs of male accessory glands. One pair is long and tubular, the other conspicuously reniform or bean-shaped. Both pairs of accessory glands, together with the seminal vesicles, empty into the ejaculatory duct at its anterior end (Gadzama, 1971; Gerber, 1976; Gadzama *et al.*, 1977).

The bean-shaped accessory glands (BAGs) produce proteinaceous and lipoproteinaceous secretions that are used in the formation of the spermatophore (Gadzama, 1971; Frenk and Happ, 1976; Dailey and Happ, unpublished). The secretion from the tubular accessory glands (TAGs), consisting of a protein–polysaccharide complex, is mixed with the fluid from the seminal vesicles in the interior of the spermatophore (Gadzama, 1971).

Both pairs of accessory glands in *T. molitor* are mesodermal in origin (Kerschner, 1913; Huet, 1966; Poels, 1972) and they first appear as organ rudiments during the prepupal stage (Poels, 1972). At this time, the oval mesodermal ampullae, derived from the vas deferens, gradually transform into the reniform shape of the BAGs, and the tubular glands arise from their ventral surfaces. During the pupal stage, the TAGs elongate. The ejaculatory

* This is part V in the series on cytodifferentiation in the accessory glands of *Tenebrio molitor*.

† Correspondence to Dr. G. M. Happ.

duct also elongates, causing the accessory glands to be moved anteriorly and the vas deferens to become coiled (Kerschner, 1913; Singh-Pruthi, 1924). Similar development has been described for the accessory glands of the elaterid beetle, *Ctenicera aeripennis destructor* (Zacharuk, 1958) which are very similar in form and probably homologous to those of *Tenebrio molitor*.

There is little detailed information about the development of the glands during the pupal stage in *T. molitor* or any other holometabolous species. This paper describes the general morphology and ultrastructure of the bean-shaped accessory glands during the 9-day pupal stage, from larval–pupal to pupal–adult ecdysis in *T. molitor*.

MATERIALS AND METHODS

Larvae of *T. molitor* were obtained from Hy-Witt Sales, Fort Lauderdale, Florida, and raised on Purina Startena chicken food and water. Newly molted pupae, distinguished by their soft, white cuticles, were collected from the cultures, sexed, and kept in an incubator at 26°C. Male pupae were aged according to the date and time of collection, and the stage of development was checked by the criteria of Delbecque *et al.* (1977) to ensure that only healthy animals with normal development were used in these investigations.

With the exception of preparations for electron microscopy, most dissections were performed in *Tenebrio* saline (Butz, 1957). Dissections for size measurements and photography of the glands were performed in 30% ethanol. The ventral cuticle was torn away and the fat body removed to expose the accessory gland complex. Measurements of glandular size (length, width, and thickness) were made with an ocular micrometer. Approximate volumes were calculated from these measurements using the formula for determination of ellipsoid volume (Burington, 1948).

For light microscopic investigations, the gland complex was fixed in alcoholic Bouin's for 1–2 hr, dehydrated in graded ethanol, cleared in xylol, and embedded in Paraplast. Sections were cut 5–8 μm thick and stained with Delafield's hematoxylin and counterstained with alcoholic eosin Y. Cell length was measured from wax sections using an ocular micrometer.

To obtain mitotic indices, pupae were injected with 2 μl of a 2% solution of colchicine (approximately 20 μg/g body weight) in *Tenebrio* saline. After 4 hr, the gland complex was dissected and processed for light microscopy as described above. Counts were made of mitotic nuclei and of total nuclei for the gland as a whole. Separate counts were made for each of 4 regions of the gland (anterior, posterior, outer edge and inner edge), so that rates of mitosis in different regions could be compared.

Estimations of glandular surface area were made by using camera lucida tracings of serial sections of the glands. The perimeters of the tracings were measured with a map measure, and surface area was calculated by multiplying by the section thickness represented by each tracing.

Comparative rates of DNA synthesis were investigated using the technique of Kurushima and Ohtaki (1975). Pupae were injected with 1 μCi of ^{3}H-thymidine in 4 μl of saline. After 4 hr, the glands were dissected free from the remainder of the complex, rinsed in cold saline, and homogenized in 1 ml cold 5% TCA. The samples were stored at 0°C for 30 min, and then poured through glass fiber filters. The filters were washed 5–6 times with cold 5% TCA (total volume of 30 ml) to remove soluble thymidine and metabolic by-products and the filters dried under a heat lamp. The dry filters were placed in 10 ml scintillation solution consisting of 16.3 g Dry Blend I (Eastman Kodak Co.) or the same weight of a mixture containing 98% PPO/2% POPOP in 4 liters of toluene. The samples were then counted for 20 min each on a Packard Tri-Carb Liquid Scintillation Spectrometer.

Tissues were dissected, minced, and fixed for 1 hr in 3% glutaraldehyde in phosphate buffer, pH 7.3. The tissue pieces were post-fixed for 45 min in 1% OsO_4 in phosphate buffer, *en bloc* stained with 2% aqueous uranyl acetate for 5 min, dehydrated in graded acetones, and embedded in Epon 812.

The sections were stained with saturated uranyl acetate in ethanol and post-stained with lead citrate (Venable and Coggeshall, 1965). Stained sections were examined on an RCA EMU3D microscope.

OBSERVATIONS

Immediately following ecdysis to the pupal stage, the accessory gland complex is located ventral to the intestine at the level of the seventh or eighth abdominal segment. The BAGs are oval (Fig. 2) and the TAGs are visible as outgrowths on the ventral surfaces of the bean-shaped glands. The accessory gland complex is moved anteriorly due to the elongation of the ejaculatory duct to which it is attached. By day 9 of the pupal stage, just before eclosion, the glands lie at the level of the second or third abdominal sternum. This change in

TABLE 1. LOCATION AND SIZE OF THE BEAN-SHAPED ACCESSORY GLANDS DURING THE PUPAL STAGE

Age (days)	Location (abdom. segment)	Approximate volume (mm^3)
0	7 – 8	0.1
1 – 2	6 – 7	0.13
3 – 4	4 – 5	0.15
5 – 7	3 – 4	0.21
8 – 9	2 – 3	0.34

Sizes were measured using an ocular micrometer. Eight to ten samples were averaged for each age, and the data were grouped and averaged for those ages exhibiting very similar glandular location and size.

position is accompanied by an increase in gland size. The BAGs grow to about 3.5 times their original volume, and the reniform shape characteristic of the adult glands becomes more pronounced (Figs. 2–6). Table 1 summarized the changes in size and location of the glands during the pupal stage. Further evidence of this growth is demonstrated by the increase in surface area of the BAGs (Fig. 7).

The BAGs consist of a single-layered columnar epithelium surrounded by several layers of muscle cells (Fig. 1). Interphase nuclei of the epithelial cells are oval with small, dispersed masses of chromatin, and these nuclei occur in the middle and basal zones of the cells. Mitotic cells are more rounded, and mitotic figures are seen exclusively in the apical region (Figs. 13, 14), a characteristic of many developing epithelia (Sauer, 1936; Glucksmann, 1964; Wessels, 1964; Zwann *et al.*, 1969; Berridge *et al.*, 1976). At the time of ecdysis (Fig. 2) to the pupa, the BAG epithelial cells are approximately 35 μm. By day 9, the cells have elongated to a height of between 50 and 120 μm (Fig. 1). The cells in the extreme posterior region, where the gland attaches to the ejaculatory duct, are about 25 μm in height.

General rates of cell division in the BAG, expressed as mitotic indices (MI), vary with age (Fig. 8). The general rate of mitosis is low just after ecdysis, but increases within the following 24 hr. The mitotic index remains fairly constant through day 4, peaks at day 5, and then rapidly declines. No mitotic figures were seen at either day 8 or 9.

The mitotic indices were determined in the 4 regions of BAG delineated in Fig. 9. Differences among the regions are summarized in Fig. 10. These differences were compared statistically ($R \times C$ tests, Sokal and Rohlf, 1969). Except at day 0, the rate of mitosis along the outer edge was significantly higher than that of the inner edge at 1, 2, 3, 4, 5, and 7 days ($\chi^2 P \leq 0.005$). The anterior region also tended to have a higher rate of cell division than the inner edge, with significant differences occurring at 2, 4, and 7 days. The posterior region of the gland generally had the lowest mitotic rate.

The incorporation of ^{3}H-thymidine into the nucleic acid fraction (presumably DNA) of the pupal gland is shown in Fig.11. Since the variances in the raw data are heterogeneous by Bartlett's test (Sokal and Rohlf, 1969), the data are plotted on a log scale. It can be seen that the incorporation of thymidine continues at a significant rate through day 9, even though no mitotic figures were observed after day 7. DNA synthesis continues after the cessation of cellular division, leading to polyploidy in the latter portion of the pupal stage.

The relationship between the rate of mitosis and ^{3}H-thymidine incorporation is illustrated in Fig. 12, plotted as the ratio of $\frac{\text{Average MI}}{\text{Average CPM}}$. This ratio is high through day 3, indicating that most or all of the DNA synthesis is associated with preparation for cell division. The

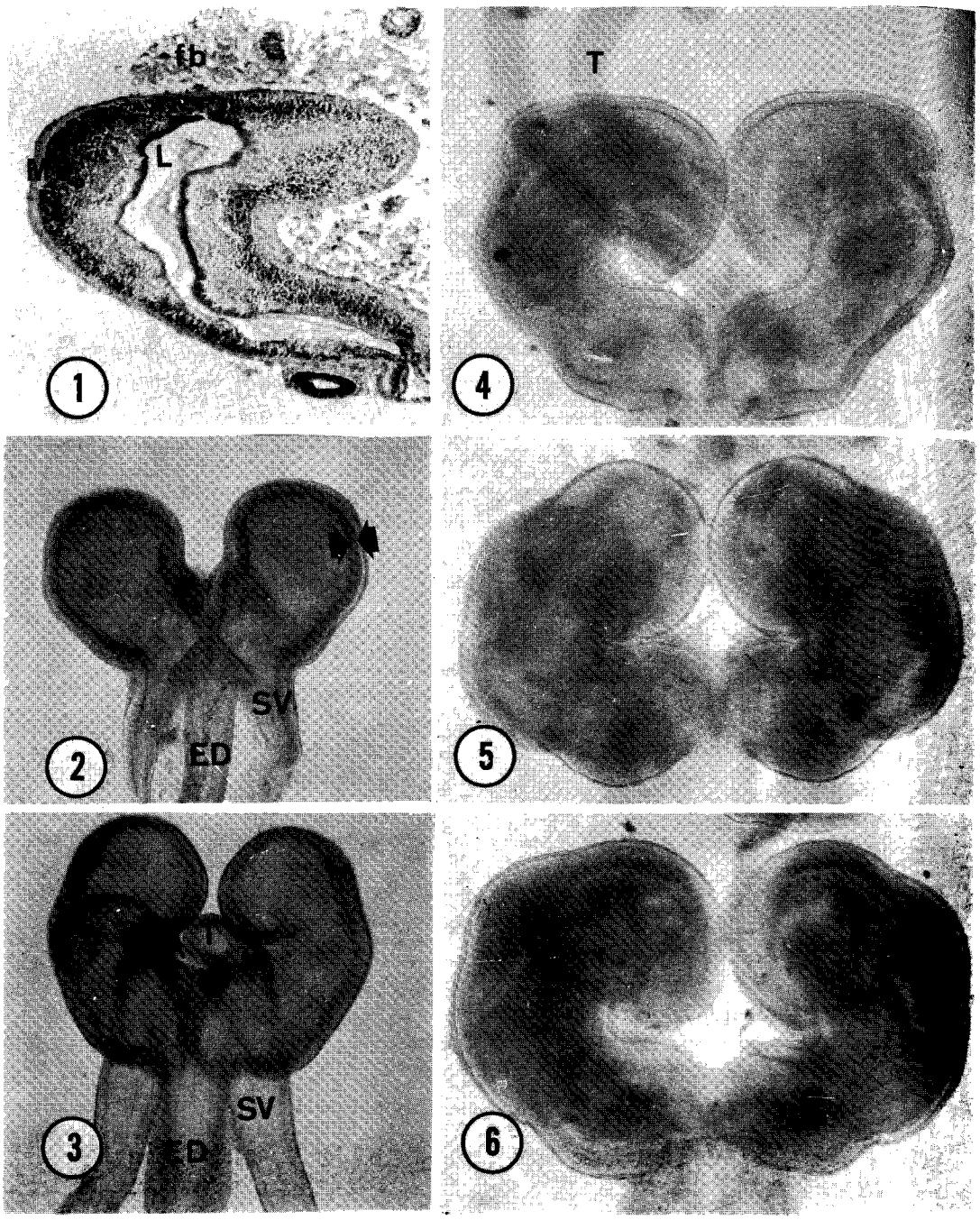

FIG. 1. Frontal section through a BAG of a 9-day pupa. Alcoholic Bouin's Haematoxylin. fb = fat body; L = lumen; M = muscle. × 100.

FIGS. 2–6. Paired pupal BAGs. Ethanol fixation, cleaned in cedarwood oil. 2. 0 day; 3. 2 days; 4. 4 days; 5. 6 days; 6. 8 days. Note thickness of epithelium (between arrows) at 0 day. ED = ejaculatory duct; SV = seminal vesicle; T = tubular accessory gland. × 50.

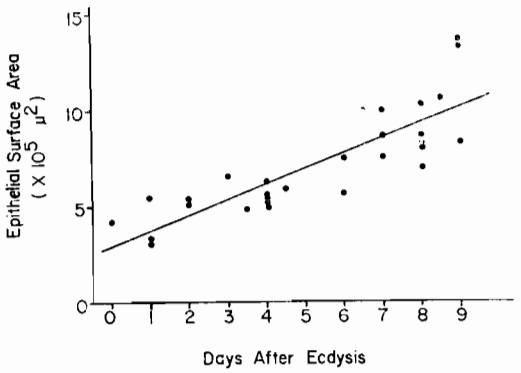

FIG. 7. Increase in epithelial surface area over pupal stage. Correlation coefficient of regression line shown is 0.837.

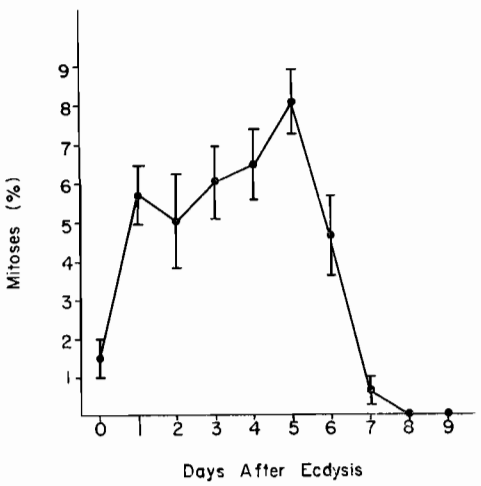

FIG. 8. Mitotic indices over pupal stage. Each age value is mean of 3–5 samples. Two standard errors are indicated by bars.

ratio then declines rapidly. It is likely that polyploidy begins as early as day 4, while some cells continue to divide through day 7.

Changes in cell ultrastructure are also seen as the accessory glands develop. In the young glands (0–4 days) (Fig. 16) the epithelial cells contain only moderate amounts of rough endoplasmic reticulum, which is distributed throughout the cytoplasm. Unbound ribosomes, most often clustered into small polysomal units, are fairly abundant. The Golgi complexes, located primarily in the perinuclear region, have both flattened and inflated lamellae, and give rise to small electron-transparent vesicles. Many mitochondria are scattered throughout the cytoplasm, although they are most numerous in the basal region. The unlobed nuclei do not have conspicuous nucleoli, and blebbing from the nuclear membrane is only rarely observed.

In interphase cells, microtubules are oriented most in anapical–basal direction. The only microtubules in mitotic cells are those associated with the spindle apparatus. Autophago-

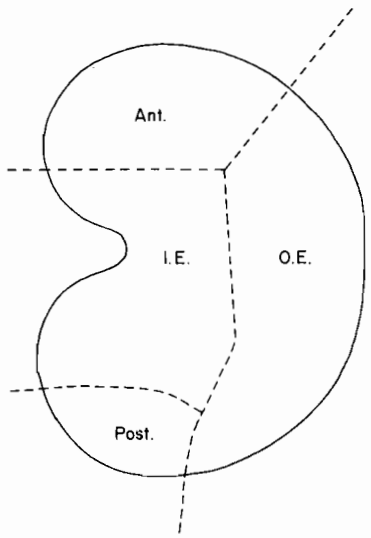

FIG. 9. Boundaries of regions counted separately to determine mitotic indices. Ant. = anterior; I.E. = inner edge; O.E. = outer edge; Post. = posterior.

somes, multivesicular bodies, and lysosome-like bodies are common features of the glandular epithelium, particularly through the first half of the pupal stage. In the apical region (Fig. 15), the cells are attached to one another by septate desmosomes, each of which is associated with zones of dense, fibrous intracellular materials. The plasma membrane adjacent to the lumen is folded to form canaliculi. More basally, the plasma membranes of apposing cells are separated by about 30-60 nm, with interspersed regions of closer apposition. The intercellular space is filled with electron-dense material (Fig. 17).

Infoldings of the plasmalemma, involving both of the apposed membranes, are commonly seen at all ages. They are abundant at 3 days. Infolding results in the formation of myelin-like figures (Fig. 16). These then break off from the plasma membrane, as they are commonly seen free in the cytoplasm.

Interruptions of the apposed plasma membranes were frequently observed (Figs. 18–20). The membranes bounding the gap between 2 cells are often vacuolated. These apposed membranes are continuous with one another, implying fusion (Figs. 17–19). The gaps, or intercellular bridges, persist after fixation in glutaraldehyde alone, osmium alone, sequential glutaraldehyde and osmium, or permanganate. We believe that these intercellular bridges are real features of the living epithelium.

The sizes of the bridges vary a great deal, sometimes extending more than 0.6 nm in length. The cytoplasm at the bridge head and within the bridge is usually indistinguishable from that of either cell, often containing ribosomes and membrane-bounded vesicles. Occasionally, the fused membranes overlap one another (Fig. 17). The bridges were more numerous during the latter part of the pupal stage, from days 4–9. The posterior region of the gland has fewer of these bridges than do the other regions.

As the glands mature, the rough endoplasmic reticulum becomes much more extensive (Fig. 21), and there are more ribosomes bound to the cisternae. Free (unbound) ribosomes and polysomes remain abundant. The nucleoli have become more noticeable by 5–6 days (Figs. 20, 24).

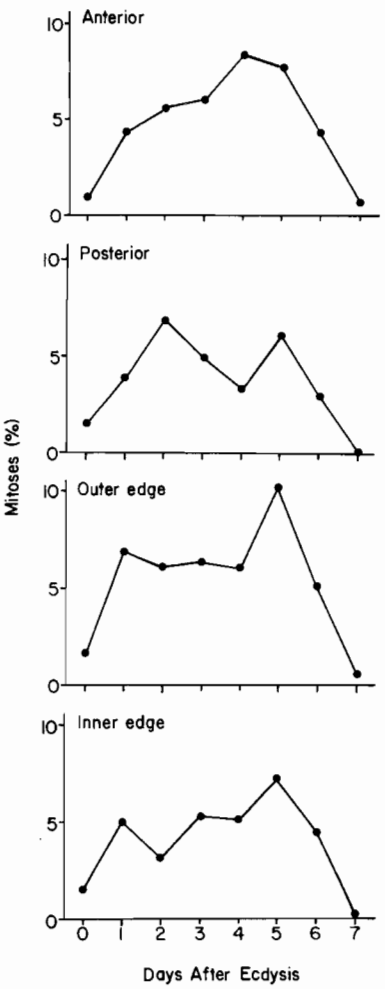

FIG. 10. Mitotic indices in regions of BAG over pupal stage.

By day 9, there is secretory activity in the BAG. Secretory product is visible in the lumen by both light and electron microscopy. The Golgi lamellae become more distended, and give rise to condensing vacuoles, containing secretory material (Fig. 22). These vesicles are most numerous in cells in the anterior region of the gland, where the product within the vesicles appears as a homogenous mass with moderate electron density (Fig. 23). The cells of the posterior region also contain a few vesicles of this type along with small numbers of vesicles that contain granular material (Fig. 25). Cells in the middle portion of the gland have larger vesicles of moderate to high electron density which might be either secretory granules or lysosomes (Fig. 26). These vesicles are near Golgi and are not seen in the apical region of the cells.

The secretory vesicles of the 9-day pupal BAG differ both in number and appearance from those in the reproductively mature adult at 6 or more days after ecdysis. The secretory vesicles of the adult BAG fall into several distinct classes (Gadzama, 1971) that cannot be distinguished in the late pupa. For example, there are no extremely electron-dense vesicles

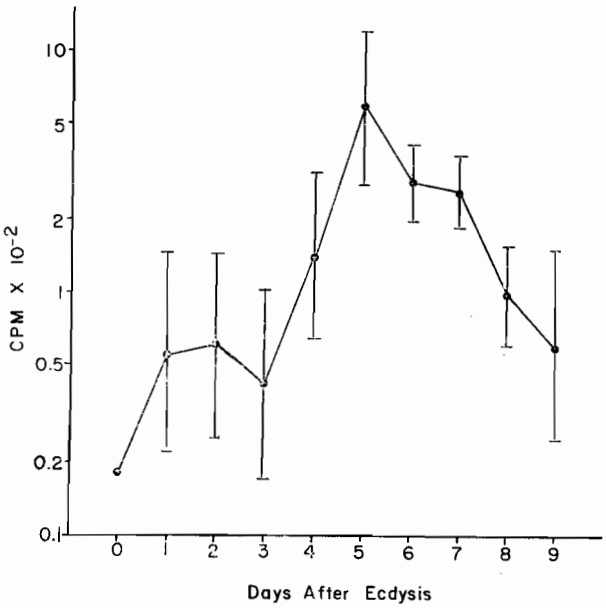

FIG. 11. ^{3}H-thymidine incorporation during pupal stage. 8–12 samples were counted at each stage. Bars are 95% confidence intervals.

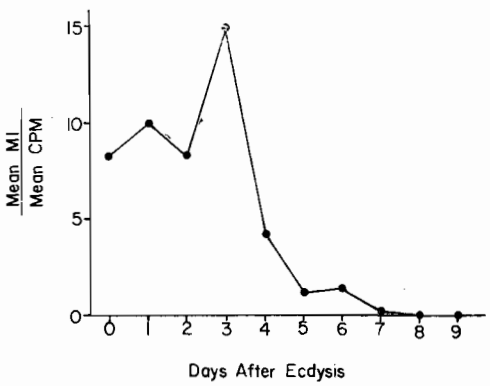

FIG. 12. Ratio of mitotic index to ^{3}H-thymidine incorporation in pupal BAG.

in the middle region of the gland and no thick-walled granules in the anterior and posterior regions, as described by Gadzama (1971).

An increase in tracheation of the BAGs also occurs during the pupal stage. In the young pupae, tracheoles were only seen in the layers of muscle surrounding the glands. By 8–9 days, tracheoles extend deep into the glandular epithelium (Fig. 24).

DISCUSSION

The differential rates of cell division seen in the BAG epithelium are probably important in the development of the reniform shape of the mature gland. The cells along the "outer edge" consistently show a higher rate of mitosis than the cells along the "inner edge." Thus, the outer edge appears to grow faster than the inner edge, causing the organ to develop

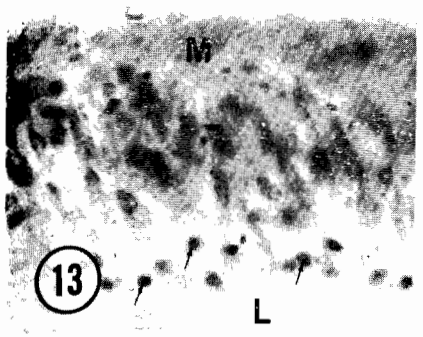

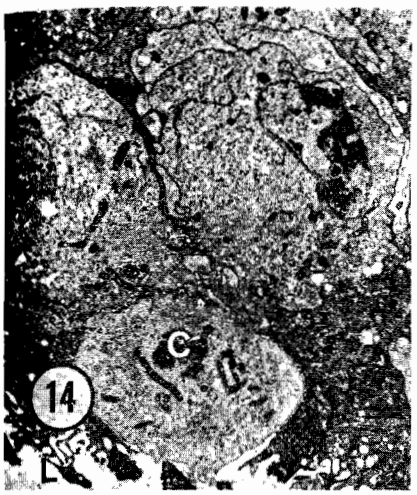

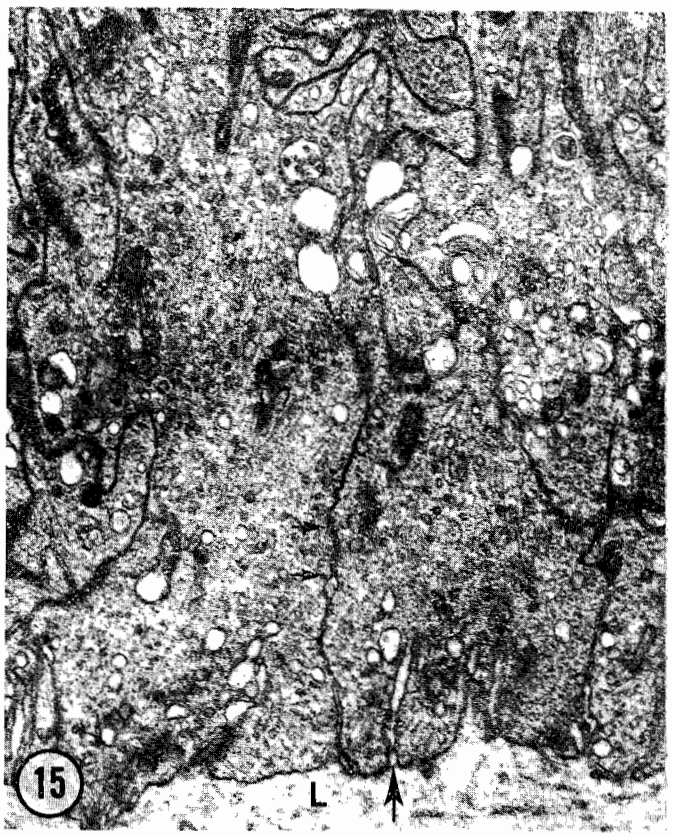

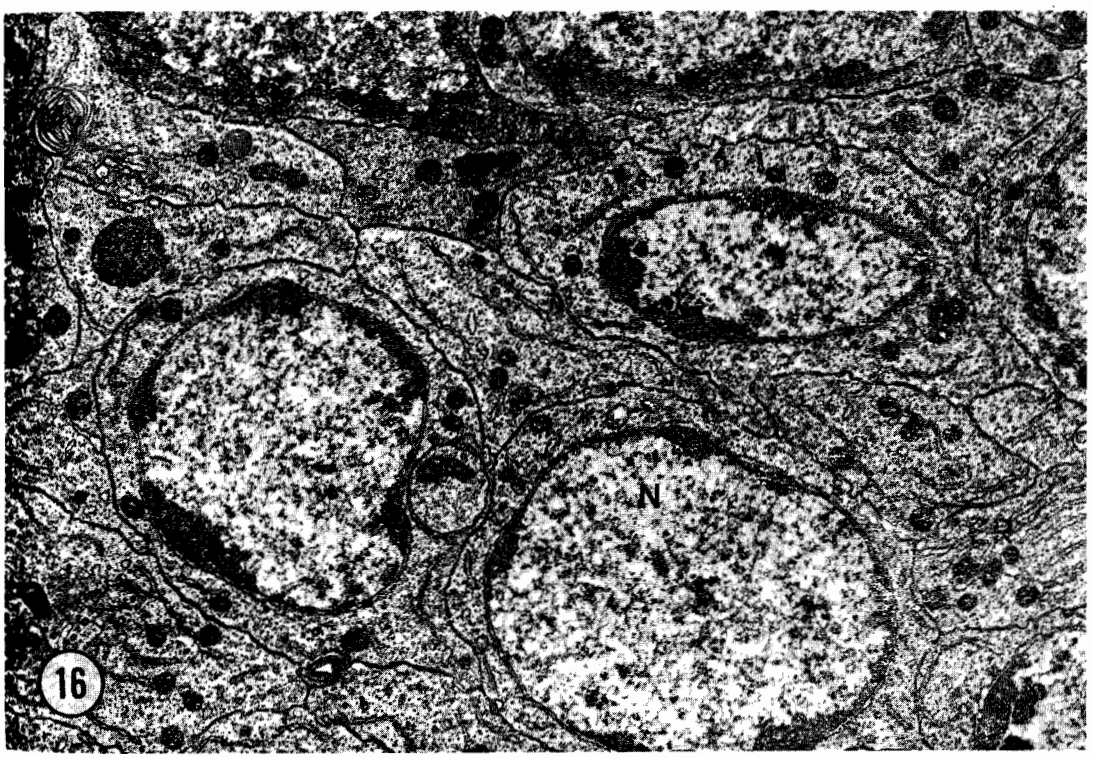

FIGS. 13–16. Captions on p. 291.

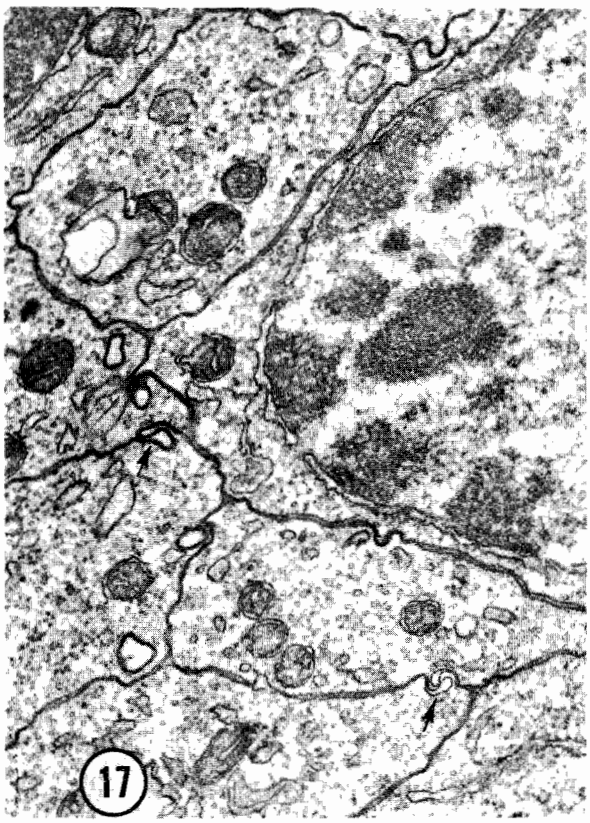
17


18

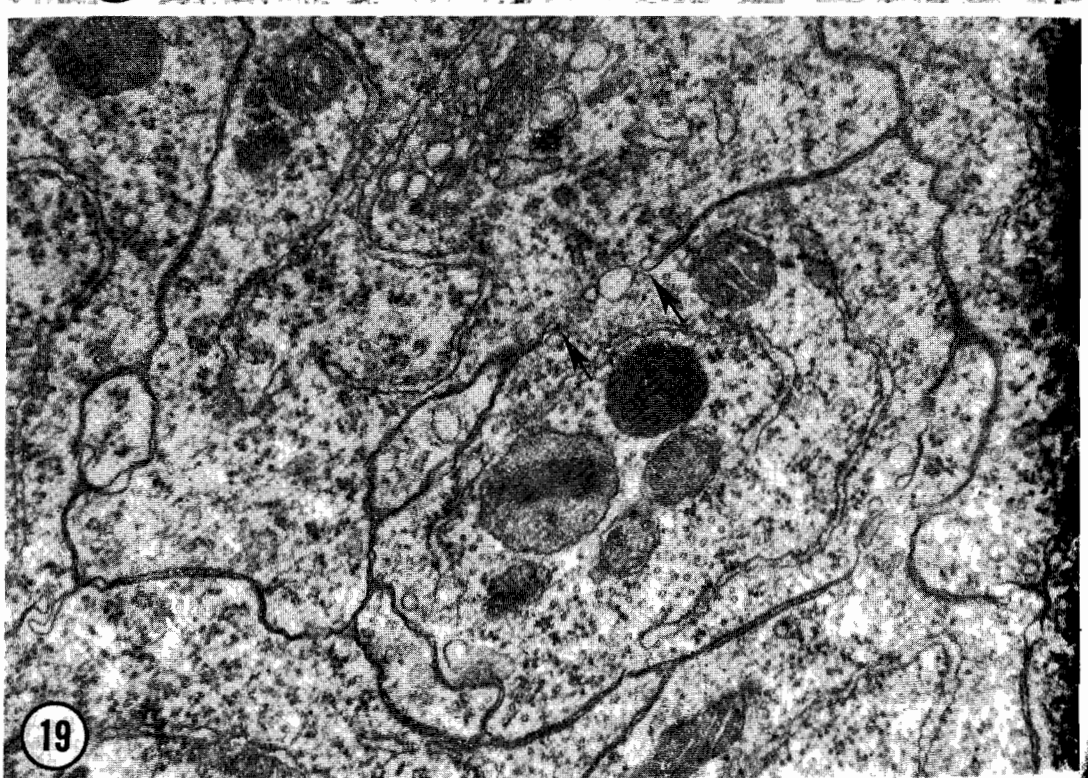
19

a curved shape, bending towards the inner edge. The anterior region also demonstrates a generally higher rate of cell division than the inner edge, assisting in the development of the curvature.

The narrowing of the gland at the posterior end is due to differential cell growth, the cells in the posterior region being much shorter than those in the other regions. Cellular elongation also plays an obvious role in the overall growth of the glands, which continues after eclosion, long after all cellular divisions have ceased.

The increase in ^{3}H-thymidine incorporation in relation to mitosis after day 3, and the continued incorporation after all mitoses have ended, indicate that the epithelial cells of the BAG become polyploid. Polyploidy is a common means of genome amplification in actively secreting gland cells, particularly in insect glands (Beermann, 1959; Gabe and Arvy, 1961; Kafatos and Feder, 1968; Kafatos, 1971; Suzuki *et al.*, 1972; Selman and Kafatos, 1974).

The synthesis of DNA may be required for further differentiation, as postulated by Ebert and Kaighn (1966). This is the case for some pupal cells of insects (Krishnakumaran *et al.*, 1967), but DNA synthesis is not a prerequisite for differentiation of many other insect cells (Selman and Kafatos, 1974, and references therein; Lawrence, 1975).

The ultrastructure of epithelial cells in the early pupal BAG resembles that of many other insect tissues that have not fully differentiated. Numerous free ribosomes, scant development of the rough endoplasmic reticulum and Golgi bodies, and moderate numbers of mitochondria are characteristic of larval imaginal discs (Agrell, 1968; Chiarodo and Denys, 1968; Ursprung and Schabtach, 1968; Poodry and Schneiderman, 1970; Greenstein, 1972; van Ruiten and Sprey, 1974), the embryonic silk gland (Tashiro *et al.*, 1976), and midgut cells in early adult development (Andries, 1975). In all of these cases, the further development of the epithelial cells yields a greater development of the rough ER and Golgi complexes.

The cytoplasmic bridges seen between adjacent BAG epithelial cells might be fixation artifacts. However, we did not observe any of these structures between healthy and pyknotic cells, and the number of bridges appeared to vary with the age and region of the gland.

FIG. 13. Section through 4-day pupal BAG following colchicine injection. Arrows indicate mitotic nuclei, arrested in metaphase, and located near lumen (L). Interphase nuclei contain disperse chromatin and are scattered in mid-zone of epithelium. M = muscle. × 815.

FIG. 14. Mitotic cells in apical region of gland at 5 days. Note spindle remnant (S) connecting 2 daughter cells at late telophase. A mass of chromatin (C) is visible in lower cell, which is dividing in a different plane of section. L = lumen. × 8000.

FIG. 15. Apical region at 7 days. Canaliculi (large arrow) extend into cells from lumen (L). Cells are attached to one another by junctions (small arrows) containing indistinct septae and associated with intracellular fibrous material. Numerous microtubules are oriented primarily in an apical-basal direction. × 19,600.

FIG. 16. Cross section through epithelium at 2 days. Cells are characterized by moderate amounts of rough endoplasmic reticulum (ER), small mitochondria, and numerous unbound polysomes. The large nuclei (N) contain no conspicuous nucleoli. My = myelin figure. × 17,100.

FIG. 17. Cross section of epithelium at 3 days. Plasma membranes of apposing cells are separated by an intercellular space containing electron-dense material. Regions of close contact and infoldings are common (arrows). × 39,930.

FIG. 18. Portions of apposing plasma membranes have fused (arrows) to form saccules probably at regions of close contact such as those seen in Fig. 17. × 47,800.

FIG. 19. Arrows indicate sizeable region of cytoplasmic continuity between cells. This intercellular bridge may be due to disappearance of saccules formed at sites of fusion as seen in Fig. 18. × 47,000.

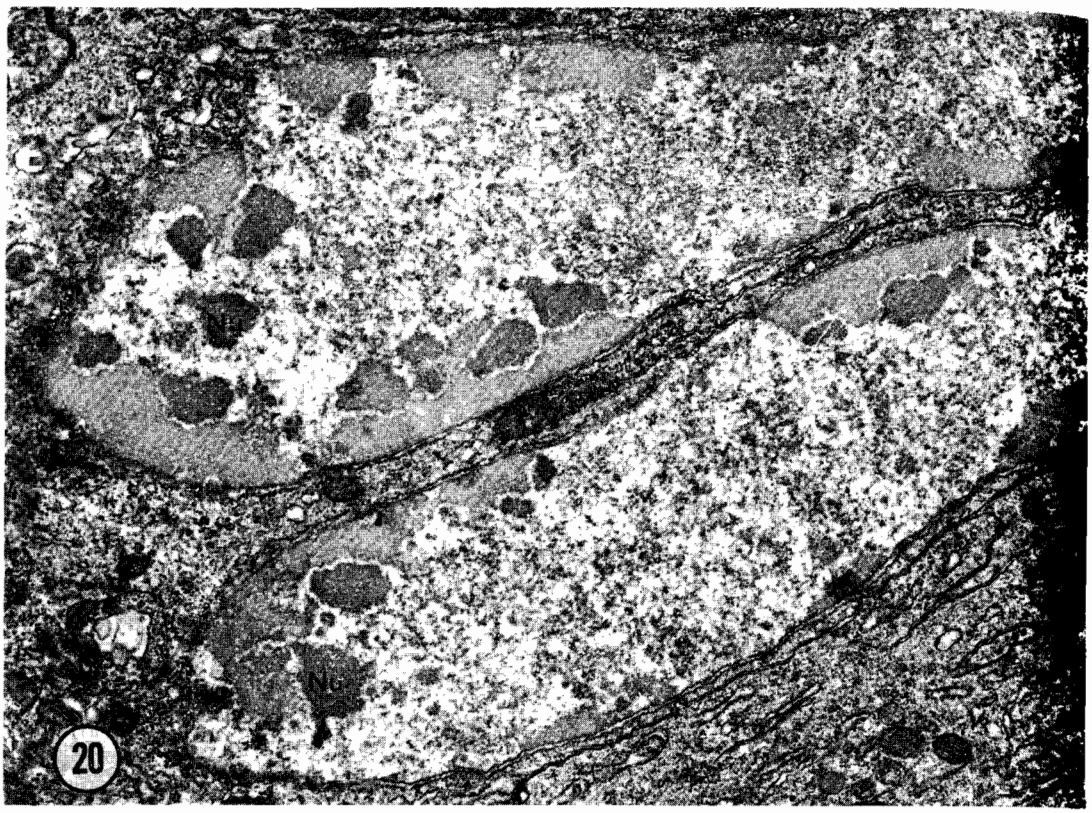

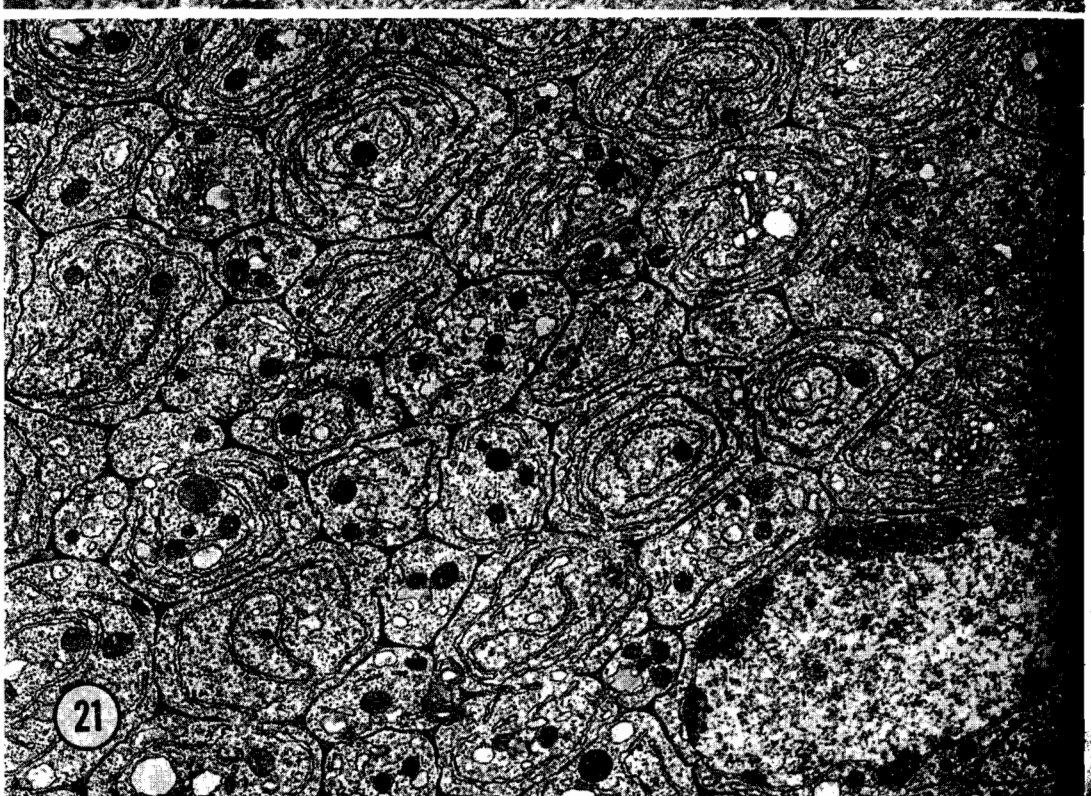

FIGS. 20 and 21. Captions on p. 294.

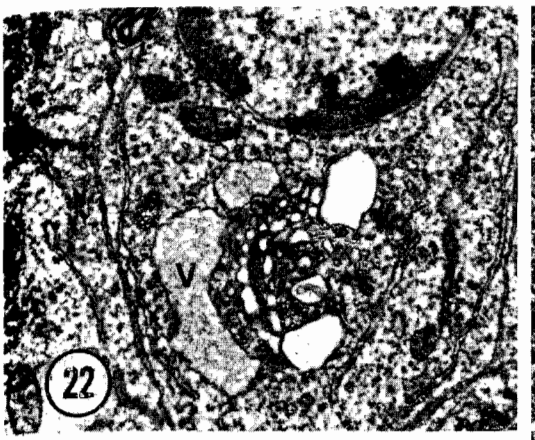

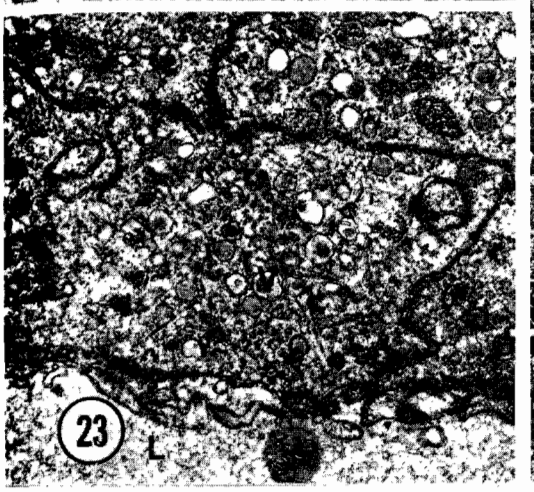

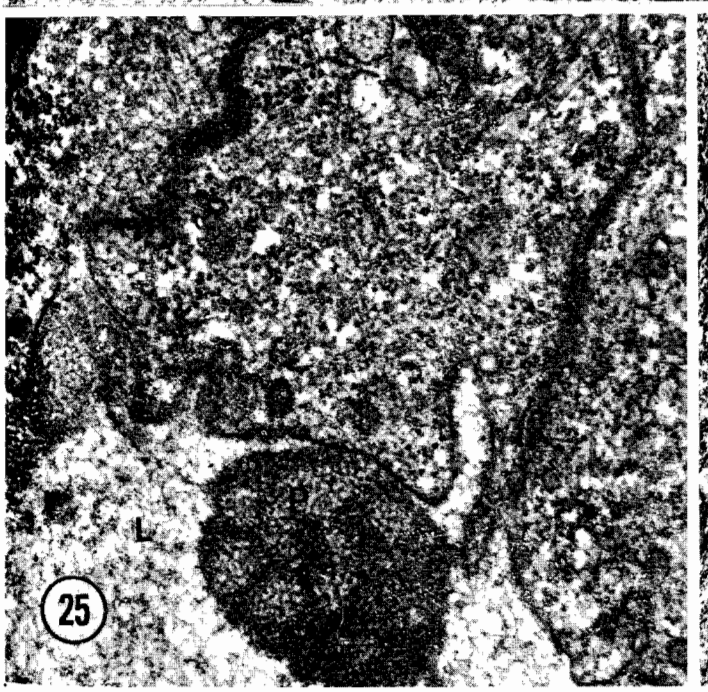

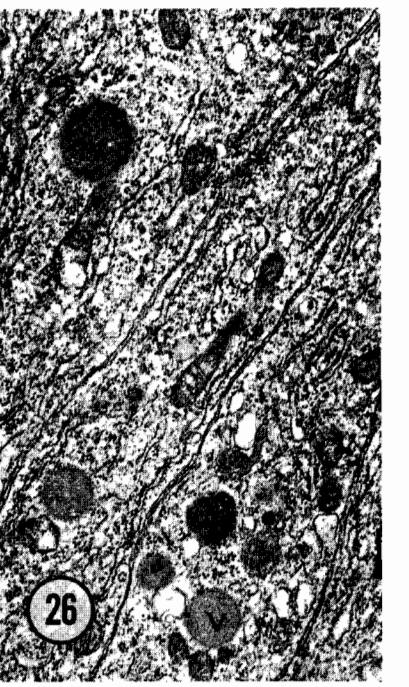

FIGS. 22–26. Captions on p. 294.

We believe that these bridges are sites of intercellular communication in the developing epithelium.

Cytoplasmic bridges similar to those seen in the BAG epithelium have been observed in the developing cerebellum of the rat (Das, 1977). These bridges are probably formed by membrane fusions at regions of close apposition as described by Shimada (1971) and Das (1977). Membrane fusions might also occur in the regions of plasmalemmal infoldings, resulting in the release of membrane-associated myelin figures into the cytoplasm. It is interesting to note that myelin figures, associated with the plasma membranes or free in the cytoplasm, were also seen in the developing salivary gland of the blow fly (Berridge *et al.*, 1976). The intercellular bridges shown in the micrographs of Berridge *et al.* (1976) resemble those seen in the BAG.

Tracheolar invaginations into the epithelium of the BAG are absent in the young glands but become very obvious by the end of the pupal stage. Tracheation of the glandular epithelium also occurs in the adult labial gland of *Antheraea pernyi* (Kafatos, 1971) and the adult vasa deferentia of *Anagasta kuhniella* (Riemann and Thorson, 1976). The appearance of these structures in the developing BAG epithelium probably reflects a higher respiratory rate in the actively secreting cells than in the less differentiated cells of the early pupa.

The regulatory signals that stimulate differentiation of the BAG epithelium are as yet unknown. The peak in ^{3}H-thymidine incorporation in the BAG closely parallels the peak of ecdysone during the pupal stage (Delbecque *et al.*, 1978), suggesting that DNA synthesis in the BAG epithelium is under hormonal control. Ecdysone has been shown to stimulate DNA synthesis in a number of tissues of saturniid moths (Bowers and Williams, 1964; Krishnakumaran *et al.*, 1967; Oberlander, 1969).

There is a temporal correlation between bursicon titres (Grillot *et al.*, 1976) and ultrastructural differentiation of the BAG epithelium. This hormone is present in low levels after day 3 of the pupal stage. An increase in bursicon titre begins at about day 7 (when the increase in the endoplasmic reticulum becomes quite noticeable), peaks at the time of eclosion (when the cells are beginning to secrete product), and declines during the first 2 days after eclosion (shortly before differentiation has been achieved). Therefore, bursicon is another putative contributor to the control of BAG differentiation.

Acknowledgements—We are grateful for support from the National Institutes of Health (NIAMD 15662 and NIGMS 26140). We thank Christine M. Happ for assistance with the drawings, Patrick Dailey for help with the light micrographs, and Warren O. Wickelgren for comments on the manuscript.

FIG. 20. Nuclei of epithelium at 6 days. Note prominence of nucleoli (Nu) and also apparent cytoplasmic continuity between cells. This tissue was fixed as usual and stained with lead citrate but not with uranyl acetate. × 22,350.

FIG. 21. Cross section through epithelium at 7 days. Rough endoplasmic reticulum is more abundant than in younger glands (c.f. Fig. 16) and cisternae are often arranged in concentric whorls. × 11,600.

FIG. 22. Golgi zone (G) in anterior region of BAG at 9 days. Large vesicles (V) contain disperse material of moderate electron density. × 24,600.

FIG. 23. Apical zone of secretory cells in anterior region of BAG at 9 days. L = lumen; P = secretory product; V = secretory vesicles. × 26,300.

FIG. 24. Mid-zone of secretory cells at 9 days. Nucleoli (Nu) are large, and tracheolar invaginations (Tr) are numerous. × 15,100.

FIG. 25. Posterior region of BAG at 9 days. Granular secretory product (P) is seen in lumen (L). × 45,500.

FIG. 26. Middle region of BAG at 9 days. V = secretory vesicles. × 24,700.

REFERENCES

AGRELL, I. P. S. 1968. Differentiation of the membrane system in the cells of imaginal discs. *Z. Zellforsch.* **88:** 365–69.

ANDRIES, J.-C. 1975. Différentiation et mort cellulaires au cours de la métamorphose mésentérique de la larve *d'Aeshna cyanea*. *J. Microsc.* (Paris) **24:** 327–50.

BEERMANN, W. 1959. Chromosomal differentiation in insects, pp. 83–103. *In* D. RUDNICK (ed.) *Developmental Cytology: The 16th Symposium of the Society for the Study of Development and Growth,* Ronald Press, New York.

BERRIDGE, M. J., B. L. GUPTA, J. L. OSCHMAN and B. J. WALL. 1976. Salivary gland development in the blowfly, *Calliphora erythrocephala*. *J. Morphol.* **149:** 459–82.

BOWERS, B. and C. M. WILLIAMS. 1964. Physiology of insect diapause. XIII. DNA synthesis during the metamorphosis of the Cecropia silkworm. *Biol. Bull.* (Woods Hole) **126:** 205–19.

BURINGTON, R. S. 1948. *Handbook of Mathematical Tables and Formulas.* Handbook Publishers, Sandusky, Ohio.

BUTZ, A. 1957. Effects of sodium, potassium, and calcium ions on the isolated heart of the mealworm, *Tenebrio molitor* L. *J. New York Entomol. Soc.* **65:** 22–31.

CHIARODA, A. J. and F. R. DENYS. 1968. Fine structural features of developing leg discs of the blowfly, *Sarcophaga bullata* (Parker). *J. Morphol.* **126:** 349–64.

DAS, G. C. 1977. Membrane-fusions and cytoplasmic bridges in the cells of the developing cerebellum. *Cell Tissue Res.* **176:** 475–92.

DELBECQUE, J.-P., M. HIRN, J. DELACHAMBRE and M. DE REGGI. 1978. Cuticular cycle and molting hormone levels during the metamorphosis of *Tenebrio molitor* (Insecta Coleoptera). *Dev. Biol.* **64:** 11–30.

EBERT, J. D. and M. E. KAIGHN. 1966. The keys to change: Factors regulating differentiation, pp. 29–84. *In* M. LOCKE (ed.) *Major Problems in Developmental Biology. 25th Symposium of the Society for Developmental Biology,* Academic Press, New York.

FRENK, E. and G. M. HAPP. 1976. Spermatophore of the mealworm beetle: Immunochemical characteristics suggest affinities with male accessory gland. *J. Insect Physiol.* **22:** 891–95.

GABE, M. and L. ARVY. 1961. Gland cells, pp. 1–88. *In* J. BRACHET and A. E. MIRSKY (eds.) *The Cell: Biochemistry, Physiology and Morphology, Vol. V.* Academic Press, New York, London.

GADZAMA, N. M. 1971. A histological, histochemical, and electron microscopical study of the spermatophore and the internal reproductive organs of male *Tenebrio molitor* L. (Coleoptera: Tenebrionidae). Ph.D. Dissertation, New York University.

GADZAMA, N. M., C. M. HAPP and G. M. HAPP. 1977. Cytodifferentiation in the accessory glands of *Tenebrio molitor*. I. Ultrastructure of the tubular gland in the post-ecdysial adult male. *J. Exp. Zool.* **200:** 211–222.

GAGE, L. P. 1974. Polyploidization of the silk gland of *Bombyx mori*. *J. Mol. Biol.* **86:** 97–108.

GERBER, G. H. 1976. Reproductive behaviour and physiology of *Tenebrio molitor* (Coleoptera: Tenebrionidae). III. Histogenetic changes in the internal genitalia, mesenteron, and cuticle during sexual maturation. *Can. J. Zool.* **54:** 990–1002.

GLUCKSMANN, A. 1964. Mitosis and degeneration in the morphogenesis of the human foetal lung *in vitro*. *Z. Zellforsch.* **64:** 101–10.

GREENSTEIN, M. E. 1972. The ultrastructure of developing wings in the giant silkmoth, *Hyalophora cecropia*. I. Generalized epidermal cells. *J. Morphol.* **136:** 1–22.

GRILLOT, J. P., J. DELACHAMBRE and A. PROVANSAL. 1976. Rôle des organes perisympathiques et dynamique de la secretion de la bursicon chez *Tenebrio molitor*. *J. Insect Physiol.* **22:** 763–80.

HUET, C. 1966. Étude expérimentale du développment de l'appareil génital mâle de *Tenebrio molitor* (Coléoptère: Ténébrionide). *C.R. Seanc. Soc. Biol.* **160:** 2021–25.

KAFATOS, F. C. 1971. Cellular metamorphosis. I. The labial gland of *Antheraea pernyi*. *Endocrinol. Exp.* **5:** 101–7.

KAFATOS, F. C. and N. FEDER. 1968. Cytodifferentiation during insect metamorphosis: The galea of silkmoths. *Science* (Wash., D.C.) **161:** 470–72.

KERSCHNER, T. 1913. Die Entwicklungsgeschichte des männlichen Copulationsapparates von *Tenebrio molitor* L. *Zool. Jahrb. Abt. Anat.* **36:** 337–76.

KRISHNAKUMARAN, A., S. J. BERRY, H. OBERLANDER and H. A. SCHNEIDERMAN. 1967. Nucleic acid synthesis during insect development. II. Control of DNA synthesis in the Cecropia silkworm and other saturniid moths. *J. Insect Physiol.* **13:** 1–57.

KURUSHIMA, M. and T. OHTAKI. 1975. Relation between cell number and pupal development of wing disks in *Bombyx mori*. *J. Insect Physiol.* **21:** 1705–12.

LAWRENCE, P. 1975. The cell cycle and cellular differentiation in insects, pp. 113–121. *In* J. REINERT and H. HOLTZER (eds.) *Results and Problems in Cell Differentiation,* Vol. 7. Springer–Verlag, Berlin, Heidelberg.

LEOPOLD, R. A. 1976. The role of male accessory glands in insect reproduction. *Annu. Rev. Entomol.* **21:** 199–221.

OBERLANDER, H. 1969. Ecdysone and DNA synthesis in cultured wing discs of the wax moth *Galleria mellonella*. *J. Insect Physiol.* **15:** 1803–06.

POELS, A. 1972. Histophysiologie des voies génitales mâles de *Tenebrio molitor* L. (Coléoptère: Ténébrionidae). *Ann. Soc. R. Zool. Belg.* **102:** 199–234.

POODRY, C. A. and H. A. SCHNEIDERMAN. 1970. The ultrastructure of the developing leg of *Drosophila melanogaster*. *Wilhelm Roux' Arch.* **166:** 1–44.

RICHARDS, O. W. and R. G. DAVIES. 1977. *Imms' General Textbook of Entomology*. Chapman and Hall, London.

RIEMANN, J. G. and B. J. THORSON. 1976. Ultrastructure of the vasa deferentia of the Mediterranean flour moth. *J. Morphol.* **149:** 483–506.

SAUER, F. C. 1936. The interkinetic migration of embryonic epithelial muclei. *J. Morphol.* **60:** 1–11.

SELMAN, K. and F. C. KAFATOS. 1974. Transdifferentiation in the labial gland of silk moths: Is DNA required for cellular metamorphosis? *Cell Diff.* **3:** 81–94.

SHIMADA, Y. 1971. Electron microscopic observations on the fusion of chick myoblasts *in vitro*. *J. Cell Biol.* **48:** 128–42.

SINGH-PRUTHI, H. 1924. On the post-embryonic development and homologies of the male genital organs of *Tenebrio molitor* L. (Coleoptera). *Proc. Zool. Soc. Lond.* **1924:** 857–68.

SOKAL, R. R. and F. J. ROHLF. 1969. *Biometry. The Principles and Practice of Statistics in Biological Research*. W. H. Freeman and Co., San Francisco.

SUZUKI, Y., L. P. GAGE and D. D. BROWN. 1972. The genes for silk fibroin in *Bombyx mori*. *J. Mol. Biol.* **70:** 637–49.

TASHIRO, Y., S. MATSUURA and K. RATA. 1976. Ultrastructural observations on the organogenesis of the posterior silk gland of the silkworm, *Bombyx mori*. *J. Insect Physiol.* **22:** 273–83.

URSPRUNG, H. and E. SCHABTACH. 1968. The fine structure of the male *Drosophila* gentital disk during late larval and early pupal development. *Wihlelm Roux' Arch.* **160:** 243–54.

VAN RUITEN, Th. M. and Th. E. SPREY. 1974. The ultrastructure of the developing leg disk of *Calliphora erythrocephala*. *Z. Zellforsch.* **147:** 373–400.

VENABLE, J. H. and R. COGGESHALL. 1965. A simplified lead citrate stain for use in electron microscopy. *J. Cell Biol.* **25:** 407–8.

WESSELS, N. K. 1964. DNA synthesis, mitosis, and differentiation in pancreatic acinar cells *in vitro*. *J. Cell Biol.* **20:** 415–33.

ZACHARUK, R. Y. 1958. Postembryonic development of the reproductive systems of the prairie grain wireworm, *Ctenicera aeripennis destructor* (Brown) (Coleoptera: Elateridae). *Can. J. Zool.* **36:** 753–77.

ZWANN, J., P. R. BRYAN, Jr. and T. L. PEARCE. 1969. Interkinetic nuclear migration during the early stages of lens formation in the chicken embryo. *J. Embryol. Exp. Morphol.* **21:** 71–83.